Cobalt-Substituted Aluminophosphate Molecular Sieves: X-ray Absorption, Infrared Spectroscopic, and Catalytic Studies

Jiesheng Chen,*,† Gopinathan Sankar,† John Meurig Thomas,*,† Ruren Xu,‡ G. Neville Greaves,§ and David Waller†

Davy Faraday Research Laboratory, The Royal Institution of Great Britain, 21 Albemarle Street, London, W1X 4BS, United Kingdom; Department of Chemistry, Jilin University, Changchun, People's Republic of China; and The SERC Daresbury Laboratory, Daresbury, Warrington, Cheshire, WA4 4AD, United Kingdom

Received July 20, 1992. Revised Manuscript Received August 7, 1992

Cobalt was incorporated by direct synthesis into three distinct kinds of microcrystalline microporous aluminophosphates (ALPOs): the large-pore ALPO-5 (free diameter ca. 7 Å), medium-pore ALPO-11 (free diameter ca. 6 Å), and small-pore ALPO-21 (free diameter <4 Å) molecular sieves. All three possess a unidimensional pore system. X-ray absorption spectroscopy (XAS) indicates that, in the CoAPO-5 and 11 precursors, the Co(II) cations are essentially four-coordinated but in CoAPO-21, which transforms into CoAPO-25 after calcination to remove the occluded template, there are some five-coordinated as well as four-coordinated framework Co(II) cations. After calcination at 550 °C in an O_2 atmosphere, the framework Co(II) cations are partly oxidized to Co(III), and once exposed to methanol they may be reduced to Co(II) cations to an extent that depends on the framework structure of the solid. The decreasing order of ease of reducibility is CoAPO-5 > CoAPO-11 ≥ CoAPO-25. Some of the tetrahedrally coordinated Co(II) species are driven out of the precursor framework and become six-coordinated during the calcination. Heteroatom-free ALPO-5, -11, and -25 contain various amounts of framework hydroxyls which function as Bronsted acid sites for the catalytic conversion of methanol to dimethyl ether. With incorporation of cobalt into its framework, ALPO-5 is able to bear hydroxyl groups with strong acidity, and as a result it catalyzes methanol conversion to hydrocarbons especially to propene. Incorporation of cobalt into ALPO-11 and ALPO-25, however, does not enhance their acidity to a comparable extent as is borne out by their catalytic performance for methanol conversion.

Introduction

Crystalline microporous solids have been used extensively as uniform heterogeneous catalysts for shape-selective conversions of hydrocarbons and alkanols.[1,2] These solids include zeolites and, more recently, the microporous aluminophosphates (ALPOs), especially their (framework) silicon and/or metal-substituted derivatives (SAPOs, MeAPOs, and MeAPSOs). Incorporation of transition-metal ions in place of Si or Al and P into the frameworks of these materials confers upon them powerful acidic properties that, in turn, may yield impressive catalytic performance.[3-6] For instance, the Ni-substituted SAPO-34[7,8] has remarkable selectivity for methanol conversion to ethene. In principle, the framework of a stoichiometric aluminophosphate molecular sieve is neutral so that it cannot bear Bronsted acid sites and it is not a good solid acid catalyst.[9] However, when a divalent metal partly substitutes the framework aluminum in an ALPO, the resulting framework becomes negatively charged and, as a result, the detacheable, extraframework protons that may then be introduced into the structure, convert the substituted ALPO into a good Bronsted acid catalyst.[4] Of the divalent metals that can replace framework aluminum, cobalt has attracted considerable attention since, in addition to the Bronsted acidity resulting from incorporation, the variable oxidation state of cobalt renders the solid a redox catalyst as well.[10] Several Co-substituted ALPOs and SAPOs[10-14] as well as ZSM-5[15-17] have been synthesized and characterized by employing a range of spectroscopic techniques. It is believed that the Co isomorphously substitutes for framework Al, but the chemical environment of the substituting Co is much in need of better definition.

In most cases, heteroatoms are incorporated into the framework somewhat randomly and dilutely, so that it is difficult to retrieve detailed information about the chemical environment of a given heteroatom by X-ray crystallography even if the substituted crystal is large enough for single-crystal structural analysis. From electron-induced X-ray emission studies, however, it is known that the heteroatoms are distributed throughout the bulk in a spatially uniform manner. X-ray absorption spectroscopy (XAS), because it is a local probe, is an effective means

† The Royal Institution of Great Britain.
‡ Jilin University.
§ The SERC Daresbury Laboratory.

(1) Thomas, J. M. *Angew. Chem., Int. Ed. Engl.* **1988**, *27*, 1673.
(2) Thomas, J. M. *Philos. Trans. R. Soc. London, A* **1990**, *333*, 173.
(3) Wilson, S. T.; Flanigen, E. M. *U.S. Patent*, **1986**, 4,567,029.
(4) Wilson, S. T.; Flanigen, E. M. *Am. Chem. Soc. Symp. Ser.* **1989**, *398*, 329.
(5) Meagher, A.; Nair, V.; Szostak, R. *Zeolites* **1988**, *8*, 3.
(6) Notari, B. *Stud. Surf. Sci. Catal.: Innovation Zeolite Mater. Sci.* **1988**, *37*, 413.
(7) Inui, T.; Phatanasri, S.; Matsuda, H. *J. Chem. Soc., Chem. Commun.* **1990**, 205.
(8) Thomas, J. M.; Xu, Y.; Catlow, C. R. A.; Couves, J. W. *Chem. Mater.* **1991**, *3*, 668.
(9) Flanigen, E. M.; Patton, R. L.; Wilson, S. T. *Stud. Surf. Sci. Catal.: Innovation Zeolite Mater. Sci.* **1988**, *37*, 13.
(10) Montes, C.; Davis, M. E.; Murray, B.; Narayana, M. *J. Phys. Chem.* **1990**, *94*, 6425.
(11) Tapp, N. J.; Milestone, n. B.; Write, L. J. *J. Chem. Soc. Chem. Commun.* **1985**, 189.
(12) Iton, L. E.; Choi, I.; Desjardins, J. A.; Maroni, V. A. *Zeolites* **1989**, *9*, 535.
(13) Kraushaar-Czarnetzki, B.; Hoogervorst, W. G. M.; Andrea, R. R.; Emeis, C. A.; Stork, W. H. J. *J. Chem. Soc., Faraday Trans.* **1991**, *87*, 891.
(14) Schoonheydt, R. A.; De Vos, R.; Pelgrims, J.; Leeman, H. *Stud. Sur. Sci. Catal.: Zeolites: Facts, Figures, Futures* **1989**, *49*, 559.
(15) Rossin, J. A.; Saldarriaga, C.; Davis, M. E. *Zeolites* **1987**, *7*, 295.
(16) Mostowicz, R.; Dabrowski, A. J.; Jablonski, J. M. *Stud. Surf. Sci. Catal.: Zeolites: Facts, Figures, Futures* **1989**, *49*, 249.
(17) Lee, K. Y.; Chou, H. *J. Catal.* **1990**, *126*, 677.

0897-4756/92/2804-1373$03.00/0

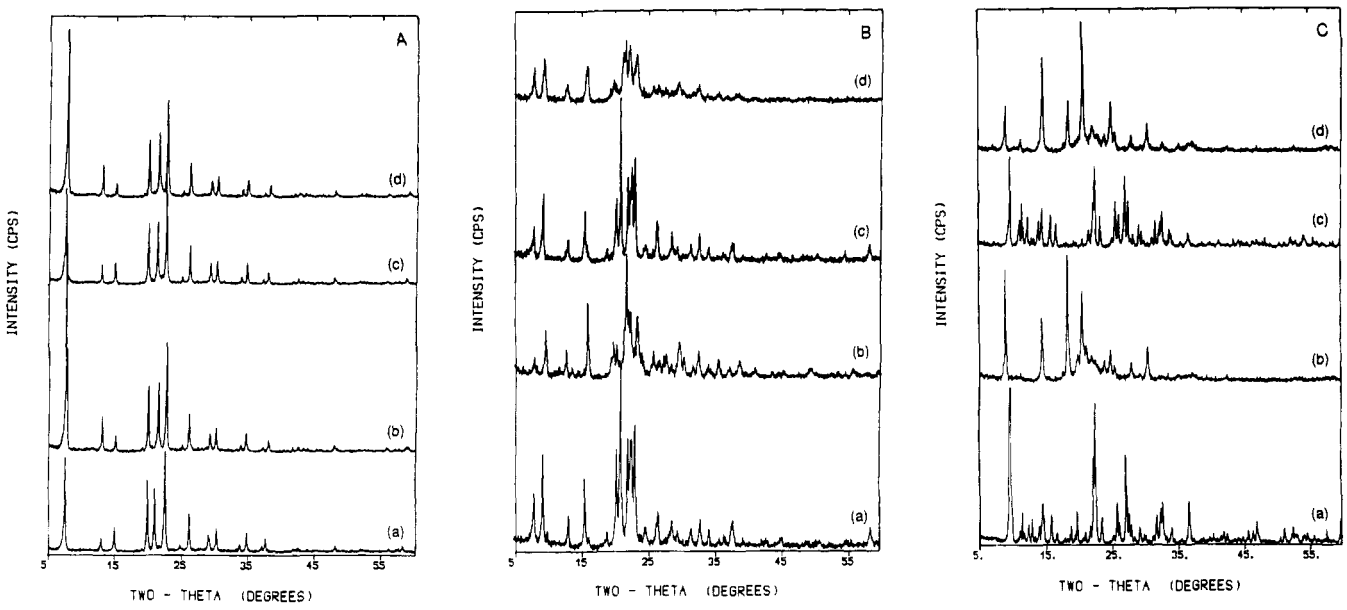

Figure 1. X-ray powder diffraction patterns: (A) (a) ALPO-5p, (b) ALPO-5c, (c) CoAPO-5p, (d) CoAPO-5c; (B) (a) ALPO-11p, (b) ALPO-11c, (c) CoAPO-11p, (d) CoAPO-11c; (C) (a) ALPO-21p, (b) ALPO-25c (c) CoAPO-21p, (d) CoAPO-25c.

of characterizing the chemical environment of a given element in both crystalline and noncrystalline materials.[18,19] XAS yields information pertaining to coordination numbers, bond lengths and angles, and the oxidation state of the absorbing element.

ALPO-5 is a large-pore molecular sieve, the framework of which has one-dimensional channels with 12-membered-ring windows (free diameter 7.3 Å).[20,21] ALPO-11 is also a unidimensional channel system, but the apertures are 10-membered rings (free diameter 3.9 × 6.3 Å);[22] it is classified as medium-pore molecular sieve. ALPO-25, which is a microporous solid transformed from its precursor ALPO-21[23] by calcination to remove the occluded template, has apertures that are eight-membered rings[24] (free diameter <4.0 Å). In this paper, we focus on the preparation of CoAPO-5, 11, 21(25), their XAS (above the Co K edge) to explore the behavior of Co atoms in all the solids, their IR spectra to probe their Bronsted acidity, and their catalytic performance for methanol conversion to ascertain their quality as solid acid (Bronsted) catalysts.[25]

Experimental Section

CoAPO-5, -11 and -21 were prepared essentially by procedures described elsewhere.[3] To obtain pure crystalline samples, we changed the recipes and reaction conditions to some degree. For CoAPO-5, a reaction mixture with composition $0.07CoO:Al_2O_3:1.3P_2O_5:1.35Et_3N:50H_2O$ was heated at 220 °C for 15 h (If the pH of the mixture was too low, dense phase $AlPO_4$ tended to form, and if the mixture pH was too high, CoAPO-34[3] appeared as an impurity in the product). The reaction mixtures for CoAPO-11 and CoAPO-21 were $0.07CoO:Al_2O_3:1.3P_2O_5:1.34$-*i*-$Pr_2NH:60H_2O$ and $0.07CoO:Al_2O_3:1.1P_2O_5:0.76(CH_2)_3(NH_2)_2:50H_2O$, respectively, where *i*-Pr_2NH is diisopropylamine and $(CH_2)_3(NH_2)_2$ is 1,3-diaminopropane. The reaction temperture for both compounds was 190 °C; the crystallization time for CoAPO-11 was 24 h and that for CoAPO-21 72 h.

To remove the templates occluded in the framework, all as-synthesized precursors were calcined at 550 °C in gaseous O_2 (1 atm) for 3 h. Afterward, the samples were exposed to air and reduced by exposure to methanol vapor at about 50–80 °C. Thereafter, the precursors are designated CoAPO-5p, CoAPO-11p, and CoAPO-21p; the calcined and air-exposed samples CoAPO-5c, CoAPO-11c, and CoAPO-25c; and the methanol-reduced ones CoAPO-5r, CoAPO-11r and CoAPO-25r, respectively.

Bulk chemical analysis gave rise to Co:Al:P ratios of 0.034:1.0:1, 0.036:1.0:1, and 0.036:1.0:1 for CoAPO-5r, CoAPO-11r, and CoAPO-21r, respectively. The Co/Al ratio in each sample was essentially the same as in the corresponding reaction mixture. However, because of the low content of Co in each sample, the results do not reflect the substitution of Co for Al rather than P in the framework.

X-ray powder diffraction was carried out on a Siemens D500 diffractometer using Cu Kα radiation. X-ray absorption measurements were made at station 7.1 of the SERC Daresbury laboratory synchrotron source. Room temperature XAS spectra were collected in the transmission geometry with a double-crystal Si[111] monochromator. CoO and Co_3O_4 were used as standards for extracting information of phase and amplitude parameters for the curve-fitting analysis of the EXAFS data of the solids. The programs for respective background subtraction and curve-fitting analysis were EXBROOK and EXCURV90 generated at the Daresbury Laboratory.[26]

Diffuse reflectance infrared Fourier transform spectra (DRIFTS) were recorded on a Perkin-Elmer 1725X FTIR spectrometer fitted with a special Spectratech attachment. The sample cell was bathed in a stream of argon during measurements; prior to measurement, samples were reheated at 500 °C for 3 h to remove occluded water. The catalytic performance for methanol conversion was tested in a quartz tube reactor. Prior to testing, the samples were activated at 450 °C for 2 h. The methanol was passed through the sample by flowing nitrogen at 1 atm; GHSV = 3000 h^{-1}. The reaction products were analyzed on a Perkin-Elmer gas chromatograph with a flame ionization detector. A Chrompack column was used to separate the products.

Results and Discussion

CoAPO-5p and 11p have essentially the same X-ray powder diffraction patterns as ALPO-5p and 11p, respectively; the pattern of CoAPO-21p is slightly different from that of ALPO-21p (Figure 1). After calcination at 550 °C to remove the template, the color of the three Co-substituted samples changes from blue to yellow (for

(18) Wong, J. *Mater. Sci. Eng.* **1986**, *80*, 107.
(19) Evans, J. In *Application of Syntrotron Radiation*; Catlow, C. R. A., Greaves, G. N., Eds.; Blackie & Son Ltd.: Glasgow, **1990**; p 201.
(20) Bennett, J. M.; Cohen, J. P.; Flanigen, E. M.; Pluth, J. J.; Smith, J. V. *Am. Chem. Soc. Symp. Ser.* **1983**, *218*, 109.
(21) Qiu, S.; Pang, W.; Kessler, H.; Guth, J. L. *Zeolites* **1989**, *9*, 440.
(22) Bennett, J. M.; Richardson, J. W., Jr.; Pluth, J. J.; Smith, J. V. *Zeolites* **1987**, *7*, 160.
(23) Parise, J. B.; Day, C. S. *Acta Crystallogr.* **1985**, *C41*, 515.
(24) Richardson, J. W., Jr.; Smith, J. V.; Pluth, J. J. *J. Phys. Chem.* **1990**, *94*, 3365.
(25) Thomas, J. M. *Sci. Am.* **1992**, *266* (4), 82 (UK Edition).
(26) Programs are available at SERC Daresbury Laboratory.

Table I. Water (25 °C, 20.0 Torr) and N_2 (−196 °C, 152 Torr) Adsorption Capacities of ALPO-5c, -11c, -25c and Their Co-Substituted Analogues

sample	ALPO-5c	ALPO-11c	ALPO-25c	CoAPO-5c	CoAPO-11c	CoAPO-25c
H_2O wt % adsorbed	18.1	12.5	4.4	9.3	8.9	4.7
N_2 wt % adsorbed	5.2	5.6		6.8	4.6	

CoAPO-11 and -21) or yellow-green (for CoAPO-5). The transformation of CoAPO-21 into CoAPO-25 was monitored on the basis of the XRD patterns. Compared with their ALPO analogues, CoAPO-5 and CoAPO-11 have less water-adsorbing capacities. On the other hand, water-adsorbing capacity of CoAPO-25 is slightly larger than that of ALPO-25 (Table I). The N_2-adsorbing capacities are not, however, quite consistent with the water-adsorbing ones. Surprisingly, CoAPO-5 has the largest N_2-adsorbing capacity among the samples measured, whereas ALPO-5, which has the largest water-adsorbing capacity, has a N_2-adsorbing capacity even less than ALPO-11. This unusual phenomenon remains a matter of further investigation. The distorted and/or blocked apertures of ALPO-25 and CoAPO-25 are too small to adsorb N_2. Their N_2 adsorption data are therefore not quoted. X-ray powder diffraction (Figure 1) shows that calcination does not influence the crystallinity of CoAPO-5p significantly but decreases that of CoAPO-11p to a certain degree; the crystallinity of CoAPO-25c is camparable with that of ALPO-25c. On reheating to remove the adsorbed water, the blue color of CoAPO-5c is restored; that of CoAPO-11c becomes grey-blue whereas there is no visible color change for CoAPO-25c. Passing methanol over the samples at 50–80 °C alters the color of CoAPO-5c to blue as well but only changes that of CoAPO-11c and 25c to grey-blue. As the blue color is characteristic of tetrahedrally coordinated Co(II),[27] we believe that the Co(III) in CoAPO-5c is easy to reduce to Co(II), whereas in CoAPO-11c and 25c it is difficult to reduce. The ease of reducibility is in the order CoAPO-5c > CoAPO-11c ≥ CoAPO-25c.

X-ray Absorption Spectroscopy. To investigate the chemical environment of cobalt in the ALPO's structures, a XAS study was applied to precursor and calcined Co-substituted samples. Since CoAPO-11c and CoAPO-25c are difficult to reduce, only the CoAPO-5r was selected for detailed XAS study along with the samples above. After calcination, the absorption threshold (see Figure 2) for each sample shifts slightly toward higher energy, reflecting the oxidation state change of Co(II) to Co(III). In parallel, the intensity of the preedge absorption, which is characteristic of tetrahedrally coordinated cobalt, decreases distinctly. Apparently, the concentration of the tetrahedrally coordinated cobalt atoms in the calcined samples is lower than in the corresponding precursor (the calcination may drive some tetrahedrally coordinated Co atoms out of the framework of each sample with consequential loss of tetrahedral symmetry). When CoAPO-5c is reduced by methanol, the absorption threshold shifts back somewhat to between that of CoAPO-5p and that of CoAPO-5c without observable change of the preedge absorption intensity. This confirms the fact that methanol does reduce the Co(III) to Co(II) but not completely.

Figure 3 shows the experimental and fitted EXAFS (extended X-ray absorption fine structure) curves and Table II lists the coordination numbers(CN) and shell distances around the Co atoms for each sample. For CoAPO-5p and -11p, the coordination numbers and Co–O distances of the first shell are quite similar. The coordination number of about four indicates that the Co(II) is

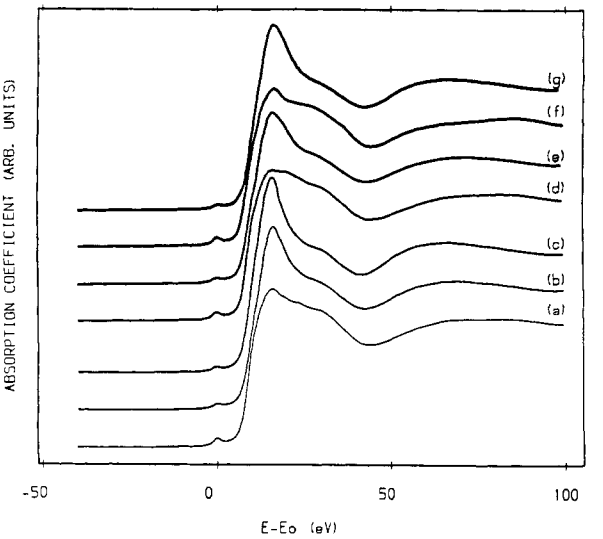

Figure 2. X-ray absorption near edge spectra (XANES): (a) CoAPO-5p, (b) CoAPO-5c, (c) CoAPO-5r, (d) CoAPO-11p, (e) CoAPO-11c, (f) CoAPO-21p, and (g) CoAPO-25c (see text).

Table II. Curve-Fitting Analysis of the EXAFS Data for Co-Substituted Aluminophosphates

	shell	CN[a]	dist (Å)	atom[b]	Debye–Waller factor
CoAPO-5p	1	4.1	1.950	O	0.009
	2	3.7	3.107	P	0.034
	3	8.1	3.602	O	0.032
CoAPO-5c	1	2.6	1.927	O	0.009
	2	2.9	2.090	O	0.009
	3	2.6	3.031	P	0.032
	4	1.9	3.211	P	0.030
	5	7.8	3.573	O	0.050
CoAPO-5r	1	2.6	1.954	O	0.008
	2	2.9	2.101	O	0.008
	3	2.6	3.056	P	0.032
	4	1.9	3.213	P	0.027
	5	7.8	3.596	O	0.047
CoAPO-11p	1	4.3	1.944	O	0.010
	2	3.7	3.078	P	0.030
	3	8.1	3.526	O	0.029
CoAPO-11c	1	2.5	1.923	O	0.009
	2	2.0	2.080	O	0.009
	3	1.9	2.972	P	0.014
	4	2.3	3.146	P	0.015
	5	4.9	3.602	O	0.026
CoAPO-21p	1	4.6	1.967	O	0.013
	2	3.8	3.068	P	0.029
	3	2.6	3.578	O	0.014
	4	4.6	4.042	O	0.037
	5	6.5	4.446	O	0.037
CoAPO-25c	1	2.2	1.913	O	0.013
	2	3.4	2.071	O	0.013
	3	1.6	2.950	P	0.020
	4	3.3	3.156	P	0.023
	5	8.1	3.557	O	0.050

[a] Coordination number. [b] P is indistinguishable from Al for the fitting.

in a tetrahedral site. The Co–O distances (1.95 Å) are also very close to those (1.93–1.95 Å) for CoO_4 tetrahedra reported earlier[28-30] on the basis of single-crystal structural

(27) Kimata, M. *Neue. Jahrbuch Miner. Abh.* **1983**, *146*, 221.

(28) Bennett, J. M.; Marcus, B. K. *Stud. Surf. Sci. Catal.: Innovation Zeolite Mater. Sci.* **1988**, *37*, 269.

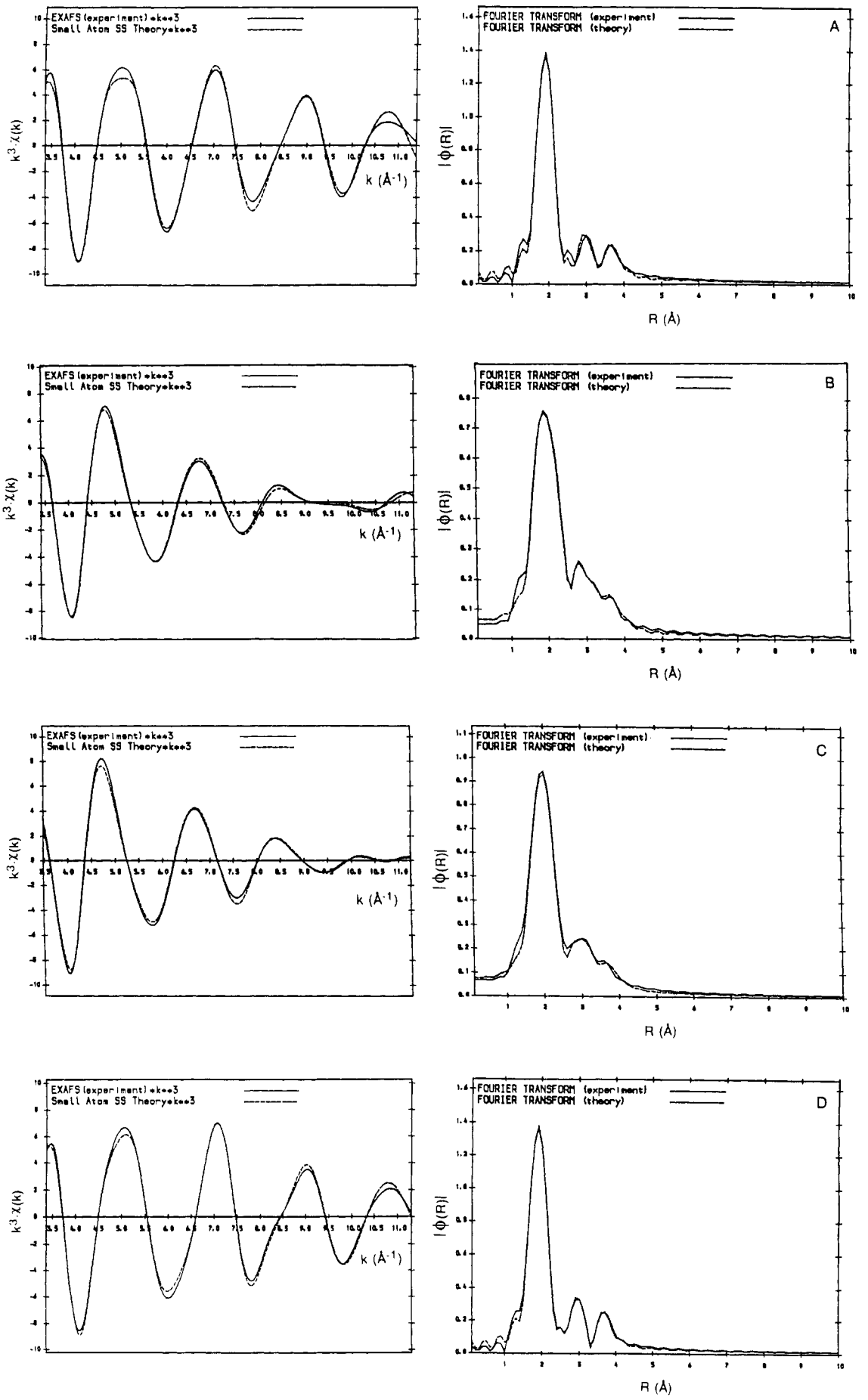

Figure 3. Experimental and fitted EXAFS: (A) CoAPO-5p, (B) CoAPO-5c, (C) CoAPO-5r, (D) CoAPO-11p, (E) CoAPO-11c, (F) CoAPO-21p, and (G) CoAPO-25c (see text).

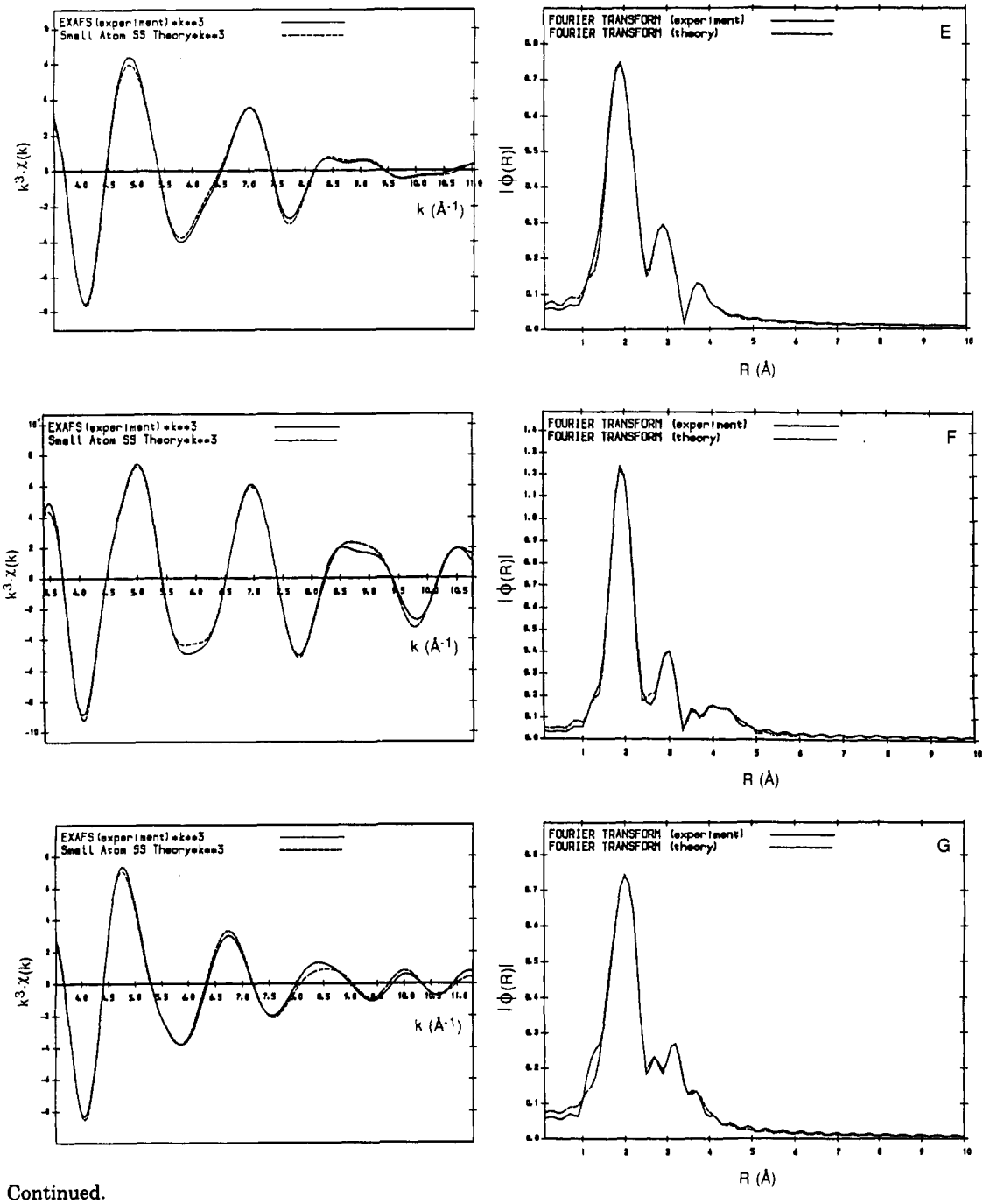

Figure 3. Continued.

analysis. These results show that almost all the Co(II) atoms have substituted the framework Al(III) tetrahedrally. Behrens and the co-workers[31] found that, in an as-synthesized CoAPO-20 with Co/Al = 0.5, there are 80% percent tetrahedrally coordinated and 20% octahedrally coordinated Co atoms. The existence of the latter can probably be attributed to the high Co concentration in their sample.

From Table II we can see that the P atoms around the Co(II) in the second shell are located at a distance of about 3.1 Å, consistent with the known crystallographic data[20,21] provided that each Co(II) has replaced one Al(II) in the framework. The atoms in the third shells are assigned to oxygen and are about 3.5 Å away from the central Co(II).

For CoAPO-21p, the coordination number (ca. 4.6) is larger and the Co–O distance (ca. 1.97 Å) longer than for CoAPO-5p and -11p. Bearing in mind that ALPO-21[23] possesses some five-coordinated Al atoms, we infer that there is Co substitution for both the four-coordinated and five-coordinated Al atoms in the framework. The P atoms in the second shell for CoAPO-21p are similar in coordination number and distance to those for CoAPO-5p and 11p. The third shell to fifth shell contain various numbers of O atoms, indicating that the non-first-shell oxygen atoms around the Co(II) in CoAPO-21p are not as uniform as in CoAPO-5p and CoAPO-11p.

After calcination, the previous first shell in each precursor splits into two new shells. The Co–O distances for CoAPO-5c are 1.927 and 2.090 Å, respectively, the latter being a typical Co–O distance for an octahedral $Co^{II}O_6$.[32,33]

(29) Roth, W. L. *J. Phys. Chem. Solids* **1964**, *25*, 1.
(30) Picard, J. P.; Baud. G.; Besse, J. P.; Chevalier, R. *J. Less-Common Met.* **1980**, *75*, 99.
(31) Behrens, P.; Felsche, J.; Niemann, W. *Catal. Today* **1991**, *8*, 479.
(32) Pizarro, J. L.; Villeneuve, G.; Hagenmuller, P.; Le Bail, A. *J. Solid State Chem.* **1991**, *92*, 273.

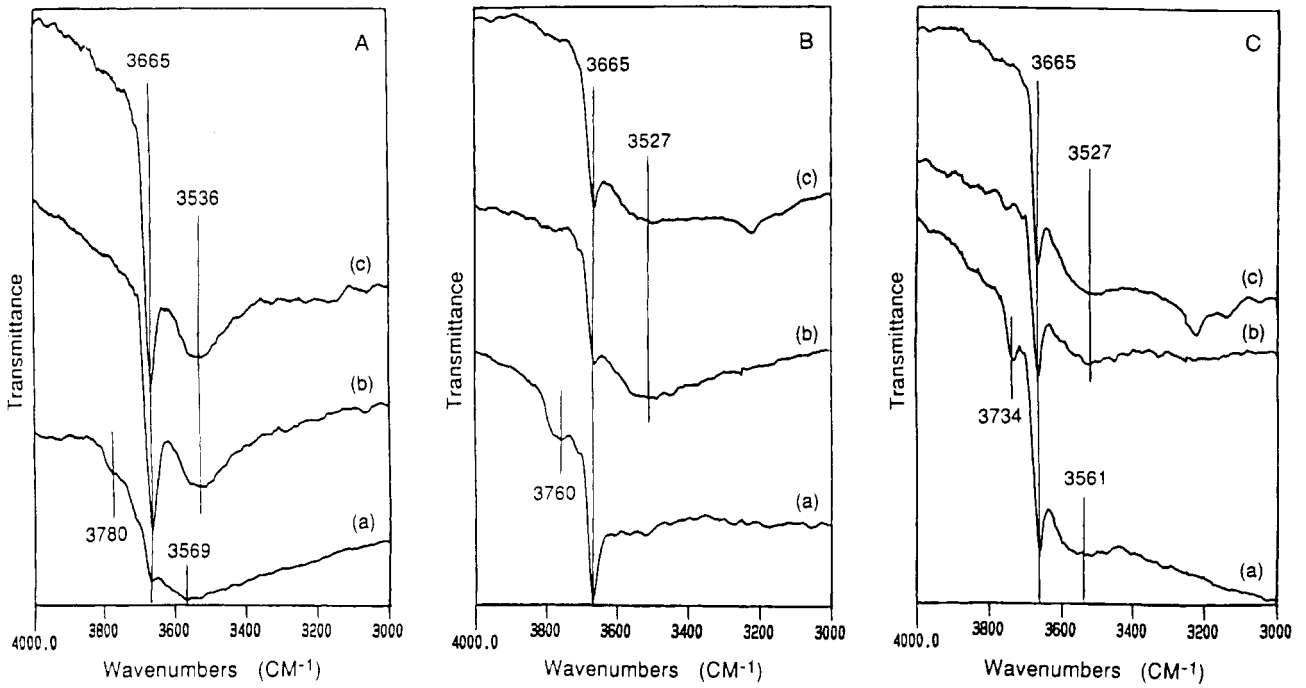

Figure 4. Diffuse reflectance infrared Fourier transform spectra (DRIFTS): (A) (a) ALPO-5c, (b) CoAPO-5c, and (c) CoAPO-5r; (B) (a) ALPO-11c, (b) CoAPO-11c, and (c) CoAPO-11r; (C) (a) ALPO-25c, (b) CoAPO-25c, and (c) CoAPO-25r.

The first Co–O distance is much shorter than the latter and even shorter than that for the tetrahedrally coordinated Co atoms in the precursor. We, therefore, conclude that the calcined sample contains at least two different types of Co species: the one with 2.090-Å Co–O distance is in an octahedral site and is believed to be outside the framework; the other should be in a tetrahedral site on the basis of the short Co–O distance. These tetrahedrally coordinated Co atoms are then believed to remain in the framework. The fact that the Co–O distance is shorter than that in the precursor suggests that the Co(II) is oxidized to Co(III) after calcination. However, the Co–O distance for a $Co^{III}O_4$ tetrahedron is about 1.89 Å[34], shorter than that found for the CoO_4 tetrahedron in CoAPO-5c. Therefore, in CoAPO-5c, there should be some $Co^{II}O_4$ tetrahedra coexisting with $Co^{III}O_4$ tetrahedra.

On the basis of the coordination numbers, we estimate that, of the total Co species in CoAPO-5c, approximately 60% are in a tetrahedral site and 40% are in an octahedral site. For CoAPO-11c and CoAPO-25c, similar phenomena are observed but the CN ratios of tetrahedra/octahedra are slightly different. There are 70% CoO_4 tetrahedra and 30% CoO_6 octahedra in CoAPO-11c, whereas CoAPO-25c has 50% CoO_4 tetrahedra and 50% CoO_6 octahedra. Since the Co–O distance for the CoO_4 tetrahedra in CoAPO-25c is 0.014 and 0.010 Å shorter than those in CoAPO-5c and CoAPO-11c, respectively, the Co(III)/Co(II) ratio in the CoO_4 tetrahedra for CoAPO-25c should be larger than for CoAPO-5c and -11c.

Affected by the split of the first shell, the second shell in the precursors occupied by P atoms correspondingly splits into two new shells in the calcined samples (see Table II). The fact that there are still P atoms around the octahedral Co(II) suggests that these Co(II) species are chemically anchored onto (but not part of) the framework. Reduction of CoAPO-5c only significantly changes the Co–O distance of the first shell, implying that the tetrahedral Co(III) in the calcined sample is reduced by methanol to tetrahedral Co(II). However, as the XANES results show (Figure 2), this reduction is not complete.

Diffuse Reflectance Infrared Fourier Transform Spectra. Figure 4 shows the DRIFTS of ALPO-5c, -11c and -25c, and their Co-substituted analogues. One sees that ALPO-5, although it should theoretically be neutral, exhibits an absorption peak at 3665 cm^{-1} and a broad one around 3569 cm^{-1}. Similar absorption bands were observed previously for various ALPO-5 samples.[35] On the basis of their sharpness, the former should correspond to isolated hydroxyl groups and the latter are attributable to hydroxyls hydrogen-bonded to framework and/or nonframework O atoms[36] (the origin and assignment of these hydroxyls is still not clear). In principle, a microporous neutral $AlPO_4$ framework should be hydrophobic just as Silicalite-I is. Surprisingly, almost all the ALPOs are hydrophilic, and the existence of hydroxyls in calcined ALPOs is itself a reflection of their hydrophilicity. ALPO-11c and ALPO-25c have an absorption feature similar to ALPO-5c except that their 3665-cm^{-1} band especially for ALPO-11c is more distinct in contrast with the low-frequency broad band. The hydrogen-bonded hydroxyl groups in ALPO-11c and 25c are clearly less intensive than those of ALPO-5c. In addition to the 3665 cm^{-1} and broad absorption bands, ALPO-5c, ALPO-11c, and ALPO-25c all have an extra absorption at 3780, 3760, and 3734 cm^{-1}, respectively; they are related to Al–OH groups.[37] CoAPO-5c and CoAPO-5r exhibit essentially the same DRIFT spectra. However, compared with ALPO-5c, their 3665-cm^{-1} band appears to be stronger and their low-frequency band becomes much sharper with its maximum shifting to about 3536 cm^{-1}, while the 3780-cm^{-1} absorption disappears.

The two absorptions observed for CoAPO-5c and CoA-

(33) Effenberger, H.; Parik, R.; Pertlik, F.; Kieck, B. *Z. Kristallogr.* **1991**, *194*, 119.
(34) Yannoni, N. F. *Doctoral Thesis*, University of Boston, **1961**.
(35) Kikhtyanin, O. V.; Paukshtis, E. A.; Ione, K. G.; Mastikhin, V. M. *J. Catal.* **1990**, *126*, 1.
(36) Senchenya, I. N.; Borovkov, V. Y. *Stud. Surf. Sci. Catal.: Catal. Adsorption Zeolites* **1991**, *65*, 653.
(37) Baumgarten, E.; Weinstrauch, F. *Spectrochim. Acta, Part A* **1979**, *35*, 1315.

Table III. Conversions for Methanol to Dimethyl Ether over ALPO-5c, ALPO-11c, and ALPO-25c

	ALPO-5c				ALPO-11c				ALPO-25c			
temp (°C)	300	350	400	450	300	350	400	450	300	350	400	450
conversion (%)	22.3	53.4	73.0	74.2	17.8	50.5	71.7	72.3	2.8	12.6	25.4	42.5

Table IV. Effect of Temperature on the Catalytic Performance of CoAPO-5r, CoAPO-11r, and CoAPO-25r for Methanol Conversion Reaction

	CoAPO-5r				CoAPO-11r				CoAPO-25r			
temp (°C)	300	350	400	450	300	350	400	450	300	350	400	450
MeOH conversion (%)	29.0	55.2	76.5	87.8	21.6	50.1	69.5	71.8	3.0	8.1	31.3	57.6
product distribution (%)[a]												
CH_3OCH_3	89.6	39.6	12.1	3.8	100	100	97.8	96.2	100	100	100	96.7
CH_4		0.5	0.5	1.0				0.5				0.9
C_2H_4	0.7	4.9	4.3	4.4								0.4
C_3H_6	3.4	25.4	32.4	41.9			1.7	2.2				1.1
C_4H_8	5.2	18.0	7.9	5.4								
C_4H_{10}		2.0	6.5	12.4								
C_{5+}[b]		9.4	36.2	31.0								

[a] Exclusive of water. [b] Including aromatic hydrocarbons.

PO-5r are more or less similar to those for SAPO-37,[38] a silico–aluminophosphate analogue of zeolite Y, except for the precise positions of the absorption bands. Because of the known existence of tetrahedral Co(II) species, it is not surprising that the reheated CoAPO-5c (or -5r) possesses a negatively charged framework, and to balance this charge, protons are produced by an appropriate mechanism. The 3636 cm^{-1} absorption may arise from the OH groups formed by the attachment of these protons to the O atoms bridging between Co and P. The disappearance of the 3780 cm^{-1} band and the intensification of the one at 3665 cm^{-1} should also be related to the incorporation of Co atoms into the framework. The DRIFTS of CoAPO-11c and CoAPO-11r are more akin to that of ALPO-5c rather than of the CoAPO-5c, except that their broad absorption bands shift toward lower frequency to 3527 cm^{-1}. Besides the 3665 cm^{-1} band and the broad band, CoAPO-11r exhibits an extra absorption at around 3222 cm^{-1} which might arise from the oxidized residue of methanol. It can be seen that, unlike CoAPO-5, the incorporation of Co into ALPO-11 does not enhance the intensity of the 3665 cm^{-1} absorption or the sharpness of the broad band and just introduces a few more hydrogen-bonded hydroxyl groups into the structure. Figure 4C also shows that the incorporation of cobalt into ALPO-25 neither improves the 3665 cm^{-1} absorption intensity nor introduces more hydrogen-bonded hydroxyls in the structure but slightly shifts the broad band toward lower frequency and causes the 3734 cm^{-1} absorption in ALPO-25c to disappear. Although both CoAPO-11c and CoAPO-25c contain considerable amount of tetrahedral $Co^{III}O_4$ (as shown by EXAFS), these species are difficult to reduce to $Co^{II}O_4$ tetrahedra, and as a result the frameworks of CoAPO-11r and CoAPO-25r are not so negatively charged as CoAPO-5r. Not many protons are present to balance the negative charges; these microporous materials contain fewer Bronsted acid sites than Co-incorporated ALPO-5.

Upon ammonia adsorption followed by heating at 300 °C for 30 min to remove the physically adsorbed ammonia, both the 3665 cm^{-1} and the broad IR absorption bands for all ALPOs and CoAPOs disappear completely. Meanwhile, the adsorbed ammonia exhibits a featureless broad band with multiple peaks between 3200 and 3400 cm^{-1}. When the samples are heated beyond 300 °C and up to 400 °C, the 3665 cm^{-1} band for each sample reappears gradually but is not completely restored, and the broad band never reappears even after heating at 450 °C for 30 min. Apparently, the hydroxyls associated with the broad band are stronger in acidity than the 3665 cm^{-1} hydroxyls.

Catalytic Performance for Methanol Conversion. Table III lists the conversions for methanol to dimethyl ether over ALPO-5c, -11c, and -25c. No appreciable amounts of hydrocarbons, which are produced only in the presence of strong Bronsted acid sites,[39] appeared in the products at all the tested temperatures. The activity of ALPO-11 is very close to that of ALPO-5. With increasing temperature, the conversions over both ALPO-5c and ALPO-11c increases from about 20% to 70%. Since ALPO-11c contains much less hydrogen-bonded hydroxyl groups on the basis of DRIFTS results, the features associated with the 3665 cm^{-1} hydroxyls clearly play an important role in the catalysis. The activity of ALPO-25c is much inferior to ALPO-5c and ALPO-11c, due partly to its low adsorption capacity (Table I). The methanol molecules can not gain full access to the acid sites, and as a result, conversions are relatively low.

Incorporation of cobalt into ALPOs improves the catalytic performance to various extents (Table IV) depending on the structures of the respective materials. Over CoAPO-5r, methanol can be converted to hydrocarbons. The selectivity of propene in the product may reach as much as ca. 42%. We believe the formation of hydroxyl groups bridging between Co and P is responsible for the improvement in catalytic performance in going from ALPO-5c to CoAPO-5r. Although CoAPO-5c has a much smaller water-adsorbing capacity than its aluminophosphate analogue (Table I), the extent of methanol conversion over the former is higher than that over the latter at each reaction temperature. On both CoAPO-11r and CoAPO-25r, only meager amounts of hydrocarbons are produced even at elevated temperatures. The total selectivity of hydrocarbons in the product over these two samples is less than 3%, and the main product is still dimethyl ether (Table IV). This is in agreement with the DRIFTS results, which reveal that both samples have few strong acid sites.

Conclusions

After removal of the occluded templates, ALPO-5, -11, and -25 contain hydroxyl groups which act as acid sites to catalyze methanol conversion to dimethyl ether and to no other product. Cobalt can be incorporated into frame-

(38) Dzwigaj, S.; Briend, M.; Shikholeslami, A.; Peltre, M. J.; Barthomeuf, D. *Zeolites* **1990**, *10*, 158.

(39) Chang, C. D. *Catal. Rev.-Sci. Eng.* **1983**, *25*, (1), 1.

works of these materials by direct synthesis. In the as-synthesized precursors of CoAPO-5 and -11, Co(II) cations substitute for the Al(III) framework cations thereby forming $Co^{II}O_4$ tetrahedra, the frameworks becoming negatively charged. In the CoAPO-21 precursor, the incorporated Co(II) occupy both four-coordinated and five-coordinated sites. After calcination in O_2 at elevated temperatures, some of the Co(II) cations are oxidized and remain in the frameworks as $Co^{III}O_4$ tetrahedra along with some unoxidized $Co^{II}O_4$ tetrahedra; the rest are driven out of and become chemically anchored onto the frameworks as $Co^{II}O_6$ octahedra. The tetrahedral $Co^{III}O_4$ species in CoAPO-5 can be readily but not completely reduced back to $Co^{II}O_4$ tetrahedra; but those in CoAPO-11 and CoAPO-25 are difficult to reduce. Since the reduction of each framework Co(III) to Co(II) introduces a proton to balance the negatively charged framework, the acidity of CoAPO-5 is greatly improved compared with that of the parent ALPO-5. CoAPO-11 and CoAPO-25, on the other hand, are not superior to their aluminophosphate analogues in acidity. CoAPO-5 is very active for methanol conversion to hydrocarbons, the predominant product being propene. The majority of the methanol conversion product on both CoAPO-11 and CoAPO-25 is dimethyl ether.

Acknowledgment. We thank SERC for general support and Unilever Plc for financial support to J.C. We are also indebted to R.H. Jones, P.A. Wright, and S. Natarajan for helpful suggestions and discussion.

Registry No. H_2O, 7732-18-5; N_2, 7727-37-9; MeOH, 67-56-1.

Photooxidation of Hexacarbonylmolybdenum(0) in Sodium Zeolite Y to Yield Redox-Interconvertible Molybdenum(VI) Oxide and Molybdenum(IV) Oxide Monomers

Saim Özkar

Chemistry Department, Middle East Technical University, 06531 Ankara, Turkey

Geoffrey A. Ozin* and Richard A. Prokopowicz

Lash Miller Chemical Laboratories, Advanced Zeolite Materials Science Group, University of Toronto, 80 St. George Street, Toronto, Ontario, Canada M5S 1A1

Received May 27, 1992. Revised Manuscript Received August 12, 1992

An analysis of the photooxidation reaction of α-cage located, site II sodium cation anchored *trans*-(ZONa)···(OC)$Mo(CO)_4$(CO)···(NaOZ) exposed to O_2 in sodium zeolite Y ($Na_{56}Y$) has been carried out using various techniques (PXRD, EXAFS, MAS/DOR-NMR, EPR, XPS, UV–vis, FTIR, gravimetry). The results have shown that it cleanly and qunatitatively converts to molybdenum(VI) oxide and CO_2 as the sole reaction products according to

$$n[Mo(CO)_6]\text{–}Na_{56}Y + {}^9/_2 nO_2 \xrightarrow{h\nu} n[MoO_3]\text{–}Na_{56}Y + 6nCO_2$$

over the full loading range $0 < n \leq 16$. Vacuum, thermally induced reductive elimination of O_2 from the molybdenum(VI) oxide photoproduct is quantitative at 400 °C and yields molybdenum(IV) oxide with no evidence for any other products having oxygen stoichiometries differing from two and three. This reduction process can be quantitatively reversed by exposure of the molybdenum(IV) oxide product to O_2 at 400 °C, according to

$$n[MoO_3]\text{–}Na_{56}Y \underset{400\ °C}{\overset{400\ °C,\ \text{vacuum}}{\rightleftharpoons}} n[MoO_2]\text{–}Na_{56}Y + {}^1/_2 nO_2$$

The structural and spectroscopic analyses demonstrate that over the loading range $0 < n \leq 16$, the aforementioned molybdenum oxides are located in the α-cages of $Na_{56}Y$ as redox-interconvertible monomers denoted (ZO)···MoO_3···(NaOZ) and (ZO)···MoO_2···(NaOZ), where ZO represents an oxygen framework six-ring or four-ring "primary" anchoring interaction and NaOZ represents a site II or site III sodium cation "secondary" interaction (the latter involving the oxygen atom of an oxomolybdenum bond). A comparison of the results for the related molybdenum and tungsten systems reveals some interesting and important similarities and differences, which are considered in terms of potential catalytic, solid-state, and materials chemistry applications envisioned for these novel kinds of molecular metal oxide nanocomposites.

Introduction

It is well-known that many molybdenum and tungsten compounds are similar in terms of their stoichiometries, structures, and chemical properties. However, there are examples of analogous compounds whose differences in properties are sometimes surprising and often difficult to explain.[1] The photooxidation of hexacarbonylmolybdenum(0) and hexacarbonyltungsten(0) contained in sodium zeolite Y turns out to be a case in point and definitely falls into this "unexpected" category. Details of the $n[W(CO)_6]\text{–}Na_{56}Y/O_2/h\nu$ system have been reported by us previously;[2-4] the analogous $n[Mo(CO)_6]\text{–}Na_{56}Y/$

* To whom correspondence should be sent.

(1) Cotton, F. A., Wilkinson, G., *Advanced Inorganic Chemistry*, 5th ed.; Wiley: New York, 1988.

0897-4756/92/2804-1380$03.00/0